ChemComm
Chemical Communications

Accepted Manuscript

This article can be cited before page numbers have been issued, to do this please use: X. Cai, J. Du, L. Zhang, Y. Li, B. Li, H. Li and Y. Yang, *Chem. Commun.*, 2019, DOI: 10.1039/C9CC06055C.

ROYAL SOCIETY OF CHEMISTRY

rsc.li/chemcomm

ChemComm

View Article Online
DOI: 10.1039/C9CC06055C

COMMUNICATION

Circularly polarized luminescence of single-handed helical tetraphenylethylene–silica nanotubes

Received 00th January 20xx,
Accepted 00th January 20xx

DOI: 10.1039/x0xx00000x

Xinye Cai,[a] Jun Du,[a] Lianglin Zhang,[a] Yi Li,[a] Baozong Li,[a] Hongkun Li*[a] and Yonggang Yang*[a]

Two single-handed helical tetraphenylethylene–silica nanotubes with circularly polarized luminescence (CPL) properties and enhanced fluorescence efficiency were fabricated through a supramolecular templating approach using the self-assemblies of chiral gelators as templates. This work provides a facile strategy for constructing CPL-active organic-inorganic hybrid nanomaterials with single-handed helical morphologies.

Circularly polarized luminescence (CPL) refers to the differential emission of left- and right-handed circularly polarized light, from which the information on the excited state of chiral luminophores can be acquired. In recent years, CPL-active materials have attracted considerable attention due to their great potential applications in chiroptical sensing[1] and optoelectronic devices,[2] including three-dimensional display, CPL laser, optical information storage and processing. Such technological applications generally require the CPL-active materials with good performance. As is known, CPL activity is usually evaluated by the luminescence dissymmetry factor (g_{lum}), $g_{lum} = 2(I_L - I_R)/(I_L + I_R)$, where I_L and I_R denote the intensities of the left- and right-handed circularly polarized luminescence, respectively. For practical use, the luminescence quantum yield, especially in the solid state, is also an important parameter for evaluating the performance of CPL-active materials.

Up to now, various CPL-active systems, such as lanthanide complexes,[1,3] organic molecules,[4] polymers,[5] liquid crystals,[6] and supramolecular assemblies,[7] have been reported. However, the CPL activities of them were mostly investigated in solutions giving the g_{lum} values in the range of 10^{-5}–10^{-2}, except for some lanthanide complexes[1] and liquid crystals.[6] From solution to aggregate state, their CPL performance generally becomes worse owing to the concentration quenching or aggregation-caused quenching effect of the conventional luminophores.[8] Exploration of new CPL-active materials with both large g_{lum} values and high emission efficiency in solid state is still a challenging task.

Recently, aggregation-induced emission (AIE) luminogens (AIEgens),[9] which are weakly or non-emissive in dilute solution, but emit strongly upon aggregation, have become good building blocks for constructing chiral functional materials with efficient CPL performance in condensed phase.[10] However, these systems generally require complicated synthesis and tedious purification procedures.[11] The exploration of new efficient CPL-active materials through simple strategies is thus highly demanded.

Our research group has developed supramolecular templating approaches to prepare single-handed helical organic–inorganic hybrid silica nanostructures by using organic self-assemblies as the templates.[12] Luminescent helical organic–inorganic hybrid nanomaterials, however, have been rarely constructed through such approaches. In this work, we report the first example of CPL-active tetraphenylethylene (TPE)-bridged polybissilsesquioxane (TPE–Silica) nanotubes with single-handed helicity. They were fabricated by using TPE-containing bis(triethoxysilane) (BTSTPE) as the precursor, and the self-assemblies of a pair of chiral cationic low-molecular-weight gelators (LMWGs), L-ValPyBr and D-ValPyBr, as the templates under basic conditions through an external templating approach (Scheme 1). Circular dichroism (CD) analysis indicated that the chirality was transferred from the chiral supramolecular templates to the TPE scaffolds. Moreover, the TPE–Silica nanotubes showed CPL activity with large g_{lum} values and high emission efficiency.

TPE has become a star AIEgen because of its facile synthesis, easy functionalization, good thermal and chemical stability, and high solid-state emission efficiency.[9] We thus employed a TPE derivative, BTSTPE, as the precursor. The detailed synthetic procedure is shown in the ESI. Briefly, it was synthesized by the McMurry coupling of 4-bromobenphenone

[a] State and Local Joint Engineering Laboratory for Novel Functional Polymeric Materials, College of Chemistry, Chemical Engineering and Materials Science, Soochow University, Suzhou 215123, P. R. China. E-mail: hkli@suda.edu.cn; ygyang@suda.edu.cn

†Electronic Supplementary Information (ESI) available: Experimental Section, ^{1}H NMR and HRMS spectra of BTSTPE (Fig. S1 and S2), TGA thermograms, WAXRD patterns, and DRCD and UV-vis spectra of TPES-*M* and TPES-*P* (Fig. S3-S5), optimized structures and HOMOs and LUMOs of BTSTPE dimer (Fig. S6 and S7), See DOI: 10.1039/x0xx00000x

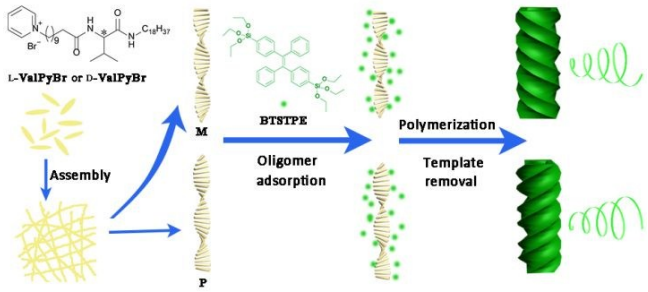

Scheme 1 The chemical structures of the chiral LMWGs of L-ValPyBr and D-ValPyBr, and the precursor of BTSTPE. Schematic illustration of the formation of single-handed helical TPE–Silica nanotubes.

followed by the silicification reaction catalyzed by $[Rh(cod)Cl]_2$[13] in an acceptable yield of 45.0%. The target compound was characterized by standard spectroscopic techniques and satisfactory analysis data were obtained (Experimental Section and Fig. S1 and S2, ESI†). The chiral LMWGs of L-ValPyBr and D-ValPyBr composed of L-valine and D-valine respectively were synthesized according to our previous reports.[14]

In our previous work, we prepared single-handed helical silica nanostructures, such as nanoribbons and nanotubes, by using tetraethoxy orthosilicate (TEOS) as the precursor and the self-assemblies of L-ValPyBr and D-ValPyBr as the templates via an external templating approach.[14] Through modification of the silicas using 4,4′-bis(triethoxysilyl)-1,1′-biphenyl (BTSB), and copolycondensation using a mixture of TEOS and BTSB as precursors respectively, the hybrid silica nanotubes with molecular chirality were obtained.[15] This inspired us to explore such an approach for fabricating CPL-active organic-inorganic hybrid nanomaterials. We employed BTSTPE as the sole precursor, and the self-assemblies of L-ValPyBr and D-ValPyBr as the templates, to prepare TPE–Silica nanostructures.

The detailed preparation process of TPE–Silica nanotubes is shown in the Experimental Section (ESI†). L-ValPyBr and D-ValPyBr are efficient gelators, which can self-assemble into left- and right-handed helical nanostructures in alcohol/water mixtures.[14] L(or D)-ValPyBr (12 mg) was readily dissolved in a 1.5 mL mixture of *n*-propanol and 10.0 wt% aqueous ammonia (7:3, v/v) under gentle heating. When the solution was cooled to 0 °C, translucent loose gels were formed and helical nanofibers were generated. BTSTPE was then dropped into the system under strong stirring. In basic conditions, the triethoxy groups of BTSTPE hydrolysed to form the hybrid silica oligomers, which were adsorbed by the pyridinium rings of the LMWGs through electrostatic interactions. The oligomers further polycondensed on the surfaces of the nanofibers. The helical nanostructures of TPE–Silica were obtained by removing the templates (Scheme 1).

The TPE–Silica samples were named as TPES-*M* and TPES-*P*, which were prepared by using the self-assemblies of L-ValPyBr and D-ValPyBr respectively as the templates. TPES-*M* and TPES-*P* are thermally stable with 5% weight loss temperatures of 505 and 486 °C, respectively, and more than 70% of their whole mass remained at 800 °C (Fig. S3, ESI†). Their thermal stability is higher than those of most of pure organic materials, which makes them promising candidates for practical applications.

The morphologies and internal pore structures of TPES-*M* and TPES-*P* were examined by field-emission scanning electron microscope (FESEM), transmission electron microscopy (TEM) and fluorescence microscope. As shown in Fig. 1a, 1b and Fig. S4 (ESI†), TPES-*M* and TPES-*P* exhibited left- and right-handed screw senses (white arrow) respectively, indicating that the morphologies of L-ValPyBr and D-ValPyBr were transcripted to the hybrid silicas.[16] The tubular structure can be identified from the terminals of the nanostructures (labelled with a red arrow in Fig. 1b) and the TEM images (Fig. 1c and 1d). The multiple nanotubes were entangled with each other. Their wall thicknesses are approximately 30–50 nm. The internal diameters of TPES-*M* and TPES-*P* are about 20 and 40–60 nm, respectively. Their helical pitches are 400–500 and 300–400 nm, respectively. Some nanotubes sealed off at the port were found, which may be caused by the adsorption of oligomers at the end of the nanotubes. Furthermore, the TPE–Silica nanotubes emit bright green fluorescence, and their length can reach tens of micrometers (Fig. 1e and 1f).

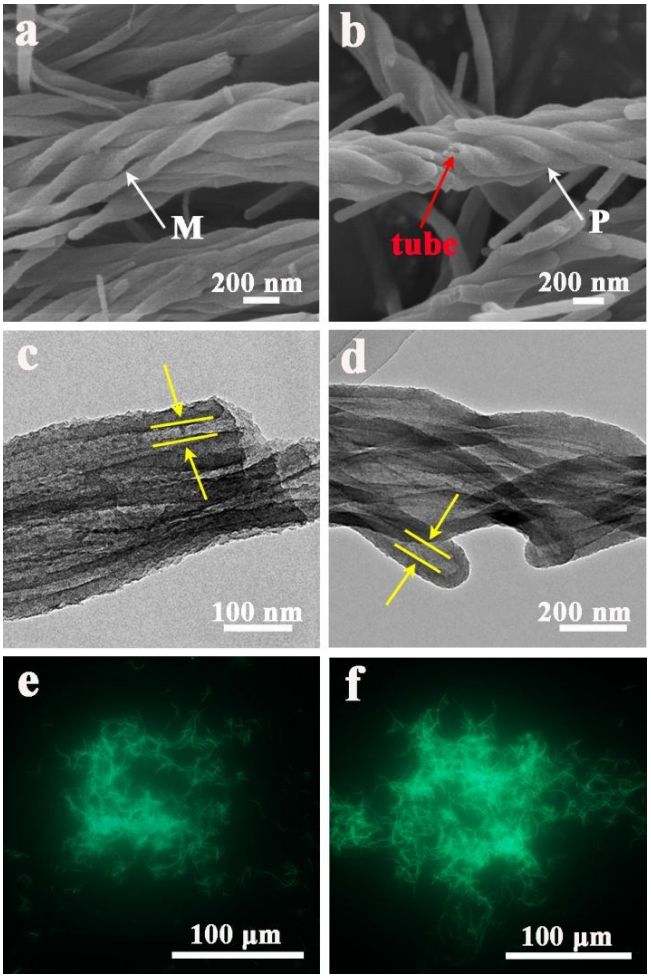

Fig. 1 FESEM (a and b), TEM (c and d) and fluorescent (e and f) images of TPES-*M* (a, c and e) and TPES-*P* (b, d and f).

In order to gain a deep understanding of the structure of the TPE–Silica nanotubes, we employed wide-angle X-ray diffraction (WAXRD) technique. Two weak and broad peaks were identified at d = 8.3 and 4.3 Å (Fig. S5, ESI†), suggesting that TPES-*M* and TPES-*P* are both amorphous materials.

Fig. 2a shows the UV-vis and CD spectra of the suspensions of the TPE–Silica nanotubes in ethanol with a concentration of 0.1 mg·mL^{-1}. They displayed the maximal absorption peaks at 322 nm, corresponding to the absorptions of the TPE units. Approximately mirror-image CD spectra were obtained for TPES-*M* and TPES-*P*. For TPES-*M*, two negative CD signals at 368 and 280 nm, and one positive CD signal at 250 nm were identified. In addition, mirror-image diffuse reflectance circular dichroism (DRCD) spectra of TPES-*M* and TPES-*P* were observed in Fig. S6 (ESI†). Two negative signals occur at 376 and 275 nm for TPES-*M*, while the opposite DRCD signals exist for TPES-*P*. The results suggest that the TPE-Silica nanotubes are chiral at molecular level, and the chirality has transferred from the self-assemblies of l-ValPyBr and d-ValPyBr.[17]

For a better understanding of the origin of the CD signals, we simulated the CD spectrum of BTSTPE dimers by using time-dependent density functional theory (TD-DFT) as well as Gaussian quantum package version, version G09. The BTSTPE dimers was structurally optimized using the B3LYP/6-31G (d) basis group, and the theoretical CD spectra was calculated by TD-DFT at the B3LYP/6-31G (d) level, which is based on 50 lowest energy singlet excited states in the calculation (Fig. S7, ESI†). We also got the corresponding molecular orbital models (Fig. S8, ESI†), in which different orbital colours represent different wave functions. When the TPE scaffolds stack in a left-handed way and its own benzene rings rotate in the left-handed manner, two positive signals appear at 379 and 278 nm and a negative signal occurs at 261 nm (Fig. 2b), which is similar to the experimental CD data of TPES-*P*. The CD signals appearing in these three regions are derived from the electronic transitions from HOMO to LUMO, HOMO-1 to LUMO+4 and HOMO-10 to LUMO, respectively. The CD signal at 379 nm originates mainly from the electronic transition between the TPE scaffolds. While the CD signal at 278 nm is mainly derived from the electronic transition in the π system of a single TPE unit. It can be found that TPES-*P* nanotubes whose TPE units stack in a left-handed manner exhibit right-handed morphology. These results demonstrate that there are no significant relationships between the chirality at the molecular-scale and the handedness at the nanoscale.[17]

Since TPE is a typical AIEgen, we then investigated the luminescence behaviours of BTSTPE and the TPE–Silica nanotubes. BTSTPE is weakly emissive in its DMSO solution. With the addition of its poor solvent of water, the emission of BTSTPE is gradually enhanced, showing AIE features (Fig. S9, ESI†). As shown in Fig. 3a, TPES-*M* and TPES-*P* powders emit green light at about 500 nm. Their fluorescence quantum yields (Φ_F) are 26.2% and 21.2% respectively, whereas the Φ_F value of their precursor of BTSTPE is 18.2%. Moreover, the fluorescence lifetimes of TPES-*M* and TPES-*P* in powder state are 5.15 and 5.17 ns, respectively, which are longer than that of BTSTPE (2.32 ns, Fig. 3b). Considering that TPE units are closely knitted together in TPES-*M* and TPES-*P*, the intramolecular motions of the phenyl rings of TPE are greatly restricted by the rigid inorganic materials, which blocks the nonradiative relaxation channel and turns on the light emission of the hybrid materials.[18] Compared with BTSTPE, a viscous liquid, the motions of phenyl rings of TPE units in the TPE-Silica nanotubes are more tightly restricted. Therefore, the luminescence efficiency and lifetime of the TPE–Silica nanotubes are both enhanced.

The intense fluorescence and molecular chirality of the hybrid materials prompted us to investigate their CPL properties. Approximate mirror images were observed in the CPL spectra of the TPE–Silica nanotubes (Fig. 3c). TPES-*M* and TPES-*P* exhibited negative and positive signals respectively, whose signs were the same as those of their CD signals. In

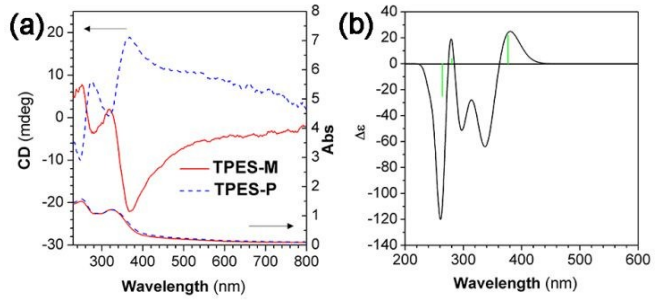

Fig. 2 The experimental CD and UV-vis spectra of TPES-*M* and TPES-*P*. (b) The simulated CD spectrum of TPE-Silica.

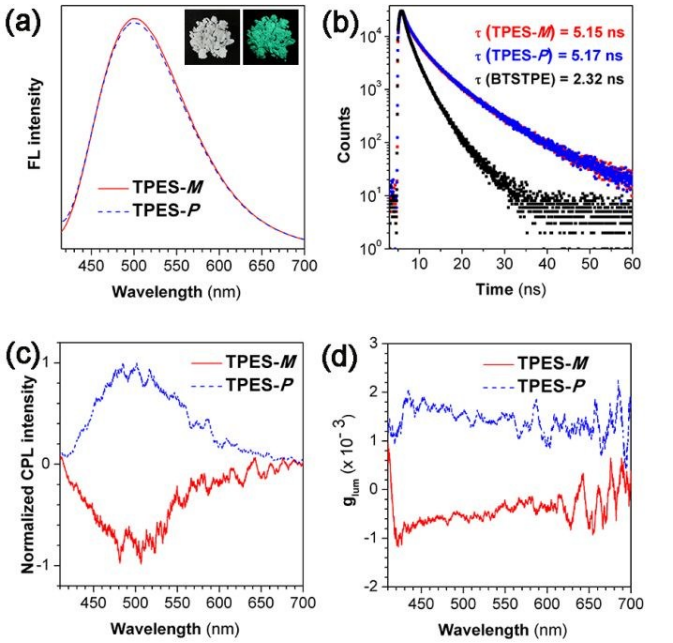

Fig.3 (a) Photoluminescence spectra of TPES-*M* and TPES-*P* powders. λ_{em}: 371 nm. Inset: Photographs of TPES-*M* under visible light (left) and 365 nm UV light (right). (b) Time-resolved fluorescence decay curves of BTSTPE, TPES-*M* and TPES-*P*. (c) Normalized CPL spectra and (d) CPL dissymmetry factor g_{lum} *versus* wavelength of TPES-*M* and TPES-*P* powders. λ_{em}: 365 nm.

other words, TPES-*M* and TPES-*P* displayed right- and left-handed CPL respectively, whose handednesses are opposite to those of the nanotubes. This further proved that there is no direct relationship between the chirality at the molecular level and the handedness at the nanolevel. The g_{lum} values of TPES-*M* and TPES-*P* were calculated to be about -0.6×10^{-3} and $+1.6 \times 10^{-3}$ at 500 nm, respectively (Fig. 3d), which were comparable to most of the CPL-active materials based on the AIEgens ($|g_{lum}| = 10^{-4} - 10^{-2}$) [10,11].

In conclusion, we have successfully prepared two single-handed helical TPE–Silica nanotubes, TPES-*M* and TPES-*P*, using BTSTPE as a single-source precursor and self-assemblies of chiral LMWGs as the templates via a supramolecular templating approach. It was found that the chirality had transferred from the templates to the inorganic- organic hybrid nanostructures. TPES-*M* and TPES-*P* exhibited CPL activities with the g_{lum} values of -0.6×10^{-3} and $+1.6 \times 10^{-3}$ respectively, and fluorescence quantum yields of 26.2% and 21.2% respectively. Additionally, they possessed high thermal stability. These properties make them promising candidates for applications in chemical sensing, CPL lasers, and photoelectronic devices. To the best of our knowledge, this is a first example of CPL-active inorganic-organic hybrid nanostructures with single-handed helical morphologies. Furthermore, this work provides a simple method for fabricating inorganic-organic hybrid functional nanomaterials with efficient CPL performance.

This work was supported by the National Nature Science Foundation of China (21875152, 51673141 and 21574095), and the Priority Academic Program Development of Jiangsu High Education Institutions (PAPD). H. Li acknowledges the financial supports from Jiangsu Planned Projects for Postdoctoral Research Funds (1501023B) and China Postdoctoral Science Foundation (2016M591906). We thank Mr. Maoxing Yu, Mr. Ruishan Huang and Prof. Zujin Zhao at the State Key Laboratory of Luminescent Materials and Devices in South China University of Technology for their kind help with the CPL and fluorescence quantum yield measurements.

Conflicts of interest

There are no conflicts to declare.

Notes and references

1 M. C. Heffern, L. M. Matosziuk and T. J. Meade, *Chem. Rev.,* 2014, **114**, 4496.

2 (a) J. Han, S. Guo, H. Lu, S. Liu, Q. Zhao and W. Huang, *Adv. Opt. Mater.,* 2018, **6**, 1800538; (b) F. Zinna, S. Voci, L. Arrico, E. Brun, A. Homberg, L. Bouffier, T. Funaioli, J. Lacour, N. Sojic and L. D. Bari, *Angew. Chem. Int. Ed.,* 2019, **58**, 6952; (c) X. Zhang, Y. Zhang, H. Zhang, Y. Li, Y. Quan and Y. Cheng, *Org. Lett.,* 2019, **21**, 439.

3 (a) M. Sugimoto, X.-L. Liu, S. Tsunega, E. Nakajima, S. Abe, T. Nakashima, T. Kawai and R.-H. Jin, *Chem. Eur. J.,* 2018, **24**, 6519; (b) N. Shi, R. Wang, X. Wang, J. Tan, Y. Guan, Z. Li, X. Wan and J. Zhang, *Chem. Commun.,* 2019, **55**, 1136.

4 (a) E. M. Sánchez-Carnerero, A. R. Agarrabeitia, F. Moreno, B. L. Maroto, G. Muller, M. J. Ortiz and S. de la Moya, *Chem. Eur. J.,* 2015, **21**, 13488; (b) Y. Nojima, M. Hasegawa, N. Hara, Y. Imai and Y. Mazaki, *Chem. Commun.,* 2019, **55**, 2749; (c) F. Pop, N. Zigon and N. Avarvari, *Chem. Rev.,* 2019, **119**, 8435.

5 (a) E. Yashima, N. Ousaka, D. Taura, K. Shimomura, T. Ikai and K. Maeda, *Chem. Rev.,* 2016, **116**, 13752; (b) T. Ikai, T. Yoshida, S. Awata, Y. Wada, K. Maeda, M. Mizuno and T. M. Swager, *ACS Macro Lett.,* 2018, **7**, 364; (c) L. Yang, Y. Zhang, X. Zhang, N. Li, Y. Quan and Y. Cheng, *Chem. Commun.,* 2018, **54**, 9663; (d) T. Yamada, K. Nomura and M. Fujiki, *Macromolecules,* 2018, **51**, 2377.

6 (a) D. Zhao, H. He, X. Gu, L. Guo, K. S. Wong, J. W. Y. Lam and B. Z. Tang, *Adv. Opt. Mater.,* 2016, **4**, 534; (b) J. Yan, F. Ota, B. A. San Jose and K. Akagi, *Adv. Funct. Mater.,* 2017, **27**, 1604529; (c) X. Li, Q. Li, Y. Wang, Y. Quan, D. Chen and Y. Cheng, *Chem. Eur. J.,* 2018, **24**, 12607; (d) X. Gao, X. Qin, X. Yang, Y. Li and P. Duan, *Chem. Commun.,* 2019, **55**, 5914.

7 (a) J. Kumar, T. Nakashima and T. Kawai, *J. Phys. Chem. Lett.,* 2015, **6**, 3445; (b) Y. Wang, X. Li, F. Li, W. Sun, C. Zhu and Y. Cheng, *Chem. Commun.,* 2017, **53**, 7505; (c) D. Yang, P. Duan, L. Zhang and M. Liu, *Nat. Commun.,* 2017, **8**, 15727; (d) T. Goto, Y. Okazaki, M. Ueki, Y. Kuwahara, M. Takafuji, R. Oda and H. Ihara, *Angew. Chem. Int. Ed.,* 2017, **56**, 2989; (e) X. Jin, D. Yang, Y. Jiang, P. Duan and M. Liu, *Chem. Commun.,* 2018, **54**, 4513; (f) F. Wang, W. Ji, P. Yang and C.-L. Feng, *ACS Nano.,* 2019, ***13***, 7281; (g) L. Ji, Y. Sang, G. Ouyang, D. Yang, P. Duan, Y. Jiang and M. Liu, *Angew. Chem. Int. Ed.,* 2019, **58**, 844.

8 J. B. Birks, Photophysics of Aromatic Molecules, Wiley, New York, 1970.

9 J. Mei, N. L. C. Leung, R. T. K. Kwok, J. W. Y. Lam and B. Z. Tang, *Chem. Rev.,* 2015, **115**, 11718.

10 (a) J. Roose, B. Z. Tang and K. S. Wong, *Small*, 2016, **12**, 6495; (b) H. Li, B. S. Li and B. Z. Tang, *Chem.-Asian J.,* 2019, **14**, 674.

11 (a) J. Liu, H. Su, L. Meng, Y. Zhao, C. Deng, J. C. Y. Ng, P. Lu, M. Faisal, J. W. Y. Lam, X. Huang, H. Wu, K. S. Wong and B. Z. Tang, *Chem. Sci.,* 2012, **3**, 2737; (b) H. Li, S. Xue, H. Su, B. Shen, Z. Cheng, J. W. Y. Lam, K. S. Wong, H. Wu, B. S. Li and B. Z. Tang, *Small,* 2016, **12**, 6593; (c) J.-B. Xiong, H.-T. Feng, J.-P. Sun, W.-Z. Xie, D. Yang, M. Liu and Y.-S. Zheng, *J. Am. Chem. Soc.,* 2016, **138**, 11469; (d) H. Qu, Y. Wang, Z. Li, X. Wang, H. Fang, Z. Tian and X. Cao, *J. Am. Chem. Soc.,* 2017, **139**, 18142; (e) H.-T. Feng, Y.-X. Yuan, J.-B. Xiong, Y.-S. Zheng and B. Z. Tang, *Chem. Soc. Rev.,* 2018, **47**, 7452.

12 (a) J. Hu and Y. Yang, *Gels,* 2017, **3**, 2; (b) Y. Li and Y. Yang, *Chem. Rec.,* 2017, **17**, 1; (c) Y. Li, S. Wang, M. Xiao, M. Wang, Z. Huang, B. Li and Y. Yang, *Nanotechnology*, 2013, **24**, 035603.

13 M. Murata, M. Ishikura, M. Nagata, S. Watanabe and Y. Masuda, *Org. Lett.,* 2002, **4**, 1843.

14 Y. Yang, M. Suzuki, S. Owa, H. Shirai and K. Hanabusa, *J. Am. Chem. Soc.,* 2007, **129**, 581.

15 F.-W. Hou, L.-M. Wu, Y.-M. Guo, Y. Li and B.-Z. Li, *Chin. Chem. Lett.,* 2013, **24**, 770.

16 (a) X. Wan, X. Pei, H. Zhao, Y. Chen, Y. Guo, B. Li, K. Hanabusa and Y. Yang, *Nanotechnology*, 2008, **19**, 315602; (b) H. Huo, Y. Li, Y. Yuan, S. Lin, B. Li, M. Wang and Y. Yang, *Chem. Asian J.*, 2014, **9**, 2866.

17 (a) H. Huo, S. Wang, S. Lin, Y. Li, B. Li and Y. Yang, *J. Mater. Chem. A*, 2014, **2**, 333; (b) X. Wu, S. Ji, Y. Li, B. Li, X. Zhu, K. Hanabusa and Y. Yang, *J. Am. Chem. Soc.*, 2009, **131**, 5986.

18 (a) J. Mei, Y. Hong, J. W. Y. Lam, A. Qin, Y. Tang and B. Z. Tang, *Adv. Mater.,* 2014, **26**, 5429; (b) D. Li and J. Yu, *Small*, 2016, **12**, 6478.

View Article Online
DOI: 10.1039/C9CC06055C

Table of Content use only

A supramolecular templating approach was employed to fabricate single-handed helical tetraphenylethylene-bridged polybissilsesquioxane nanotubes with circularly polarized luminescence activity.